

473 1 Supplementary Information

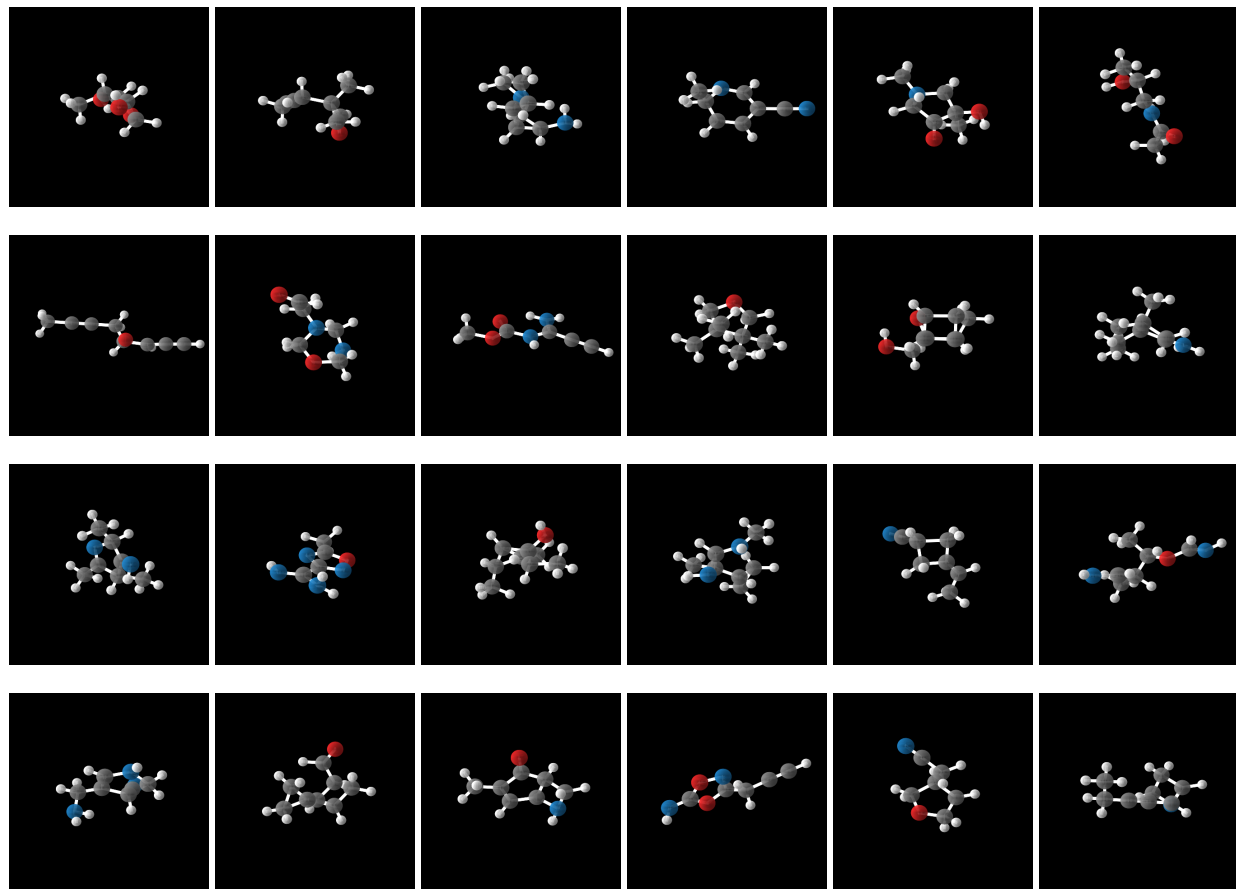


Figure S1. Randomly sampled molecules generated by MolCode trained on QM9.

Table S1. Substructure analysis of the generated molecules. The KL divergence of the bond lengths (upper part) and bond angles (lower part) between the training set and the generated molecules are shown below.

Distances/Angles	E-NFs ⁶⁰	G-SchNet ²⁴	G-SphereNet ⁴³	EDM ⁴²	MolCode (w/o bond)	MolCode
CC	0.53	0.44	0.30	0.36	0.32	0.24
CN	0.87	0.68	0.45	0.37	0.43	0.30
CO	0.49	0.32	0.24	0.26	0.25	0.21
NO	0.39	0.27	0.20	0.24	0.19	0.17
CCC	1.25	0.96	0.65	0.48	0.66	0.25
CCO	0.98	0.85	0.41	0.33	0.47	0.23
CNC	1.44	1.37	0.71	0.56	0.64	0.42
CCN	1.30	0.95	0.74	0.84	0.62	0.37

Table S2. Properties of the test set molecules and the generated molecules by different methods in structure-based drug design (the upper part shows the results of baselines and the test set; the lower part shows MolCode and its variants). We report the means and standard deviations. The best results are bolded.

Method	Vina Score (kcal/mol, ↓)	High Affinity(↑)	QED (↑)	SA (↑)	LogP	Lip. (↑)	Sim. (↓)	Div. (↑)
Testset	-7.143±1.76	-	0.477±0.18	0.642±0.17	0.924±2.06	4.443±1.18	-	-
LiGAN ⁷⁴	-6.184±0.96	0.146±0.16	0.240±0.17	0.482±0.13	-0.125±2.48	4.146±1.29	0.412±0.17	0.580±0.09
AR ⁴⁴	-6.237±1.24	0.188±0.18	0.581±0.13	0.640±0.17	0.232±1.78	4.662±0.54	0.423±0.18	0.733±0.11
GraphBP ⁴⁶	-6.368±1.65	0.236±0.15	0.454±0.20	0.459±0.18	0.512±2.13	4.574±0.44	0.413±0.11	0.687±0.15
Pocket2Mol ⁴⁷	-7.206±1.82	0.544±0.14	0.649±0.16	0.704±0.18	1.134±1.88	4.905±0.14	0.388±0.21	0.650±0.16
MolCode	-7.412±1.74	0.618±0.15	0.652±0.19	0.708±0.16	1.225±2.16	4.924±0.08	0.371±0.20	0.693±0.14
w/o check	-7.076±1.48	0.472±0.13	0.663±0.15	0.664±0.15	1.054±1.85	4.912±0.12	0.382±0.19	0.686±0.12
w/o bond	-6.895±1.67	0.414±0.14	0.620±0.17	0.642±0.13	0.926±1.93	4.829±0.18	0.390±0.21	0.676±0.16

474 In Table S2, we show more qualitative evaluations of the generated ligand molecules in structure-based drug design. We
475 choose metrics that are widely used in previous works^{44,46,47} to evaluate the qualities of the sampled molecules: (1) **Vina Score**
476 measures the binding affinity between the generated molecules and the protein pockets; (2) **High Affinity** is calculated as the
477 percentage of pockets whose generated molecules have higher affinity to the references in the test set; (3) **QED**⁶⁸ measures how
478 likely a molecule is a potential drug candidate; (4) **Synthesizability (SA)** represents the difficulty of drug synthesis (the score is
479 normalized between 0 and 1 and higher values indicate easier synthesis); (5) **LogP** is the octanol-water partition coefficient
480 (LogP values should be between -0.4 and 5.6 to be good drug candidates⁸²); (6) **Lipinski (Lip.)** calculates how many rules the
481 molecule obeys the Lipinski's rule of five⁸³; (7) **Sim.** represents the Tanimoto similarity⁸⁴ with the most similar molecules in
482 the training set; (8) **Diversity (Div.)** measures the diversity of generated molecules for a binding pocket (It is calculated as 1 -
483 average pairwise Tanimoto similarities). In our work, The Vina Score is calculated by QVina^{69,70} and the chemical properties
484 are calculated by RDKit^{71,72} over the valid molecules. Before feeding to Vina, all the generated molecular structures are firstly
485 refined by universal force fields⁷³. To sample molecules, we apply 5 independent runs with random seeds.

Table S3. Results of random molecule generation on GEOM-Drugs. We follow the preprocessing procedure in previous work⁷⁶. Validity calculates the percentage of valid molecules among all the generated molecules; Uniqueness refers to the percentage of unique molecules among the valid molecules; Novelty measures the fraction of molecules not in the training set among all the valid and unique molecules. Time records the sampling time for 10,000 molecules. The best results are bolded.

Method	Validity	Uniqueness	Novelty	Time
G-SphereNet ⁴³	39.16%	96.45%	98.70%	2746
EDM ⁴²	44.71%	100.00%	100.00%	25284
MolCode (w/o check)	72.30%	98.75%	97.43%	3162
MolCode (w/o bond)	63.46%	98.14%	98.77%	3488
MolCode	98.82%	100.00%	100.00%	3950

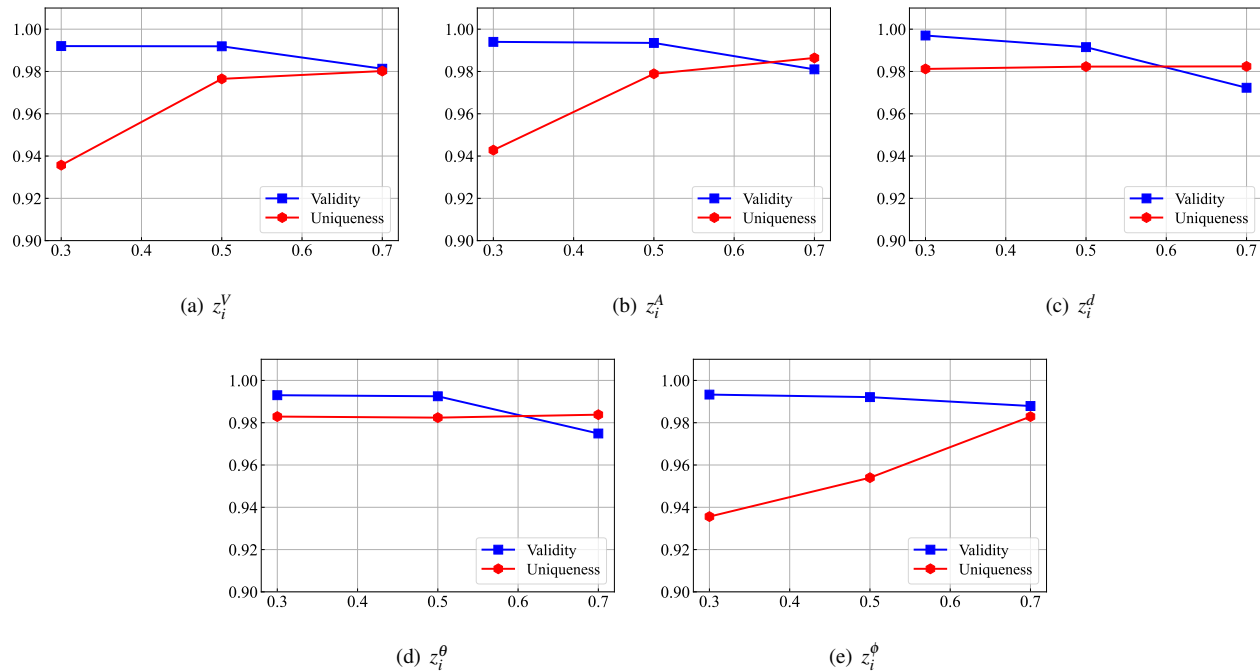


Figure S2. Influence of temperature hyperparameters on Validity and Uniqueness in the random molecule generation task.

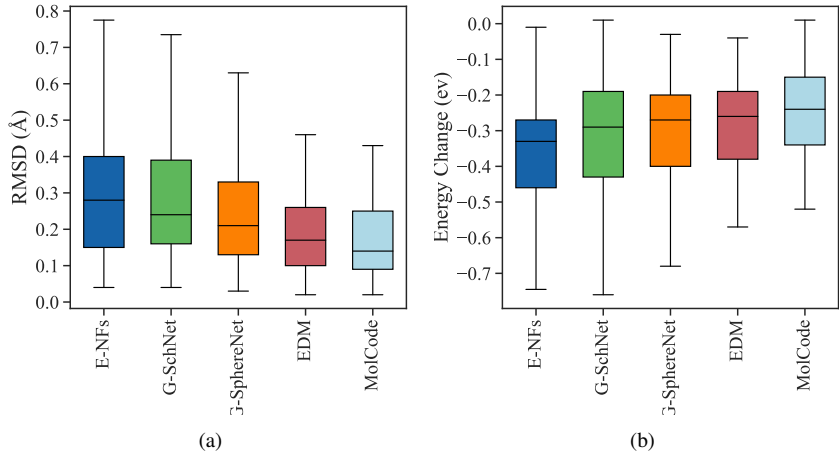


Figure S3. (a) The RMSD of the atomic positions between the generated and the corresponding relaxed molecules with force fields. Following previous works on molecular conformation generation^{38,85}, we use the empirical force field⁸⁶ to optimize molecular conformations. (b) The internal energy change between the generated and the corresponding relaxed molecules ($E_{\text{relaxed}} - E_{\text{generated}}$). Following cG-SchNet²⁶ and G-SchNet²⁴, we use the pretrained SchNet models from SchNetPack⁸⁸ to predict the internal energy at zero Kelvin of generated molecules.

Algorithm 1 Training Algorithm of MolCode

Input: Molecular dataset \mathcal{M} , learning rate η , Adam hyperparameters β_1, β_2 , batch size B , GoGen model with trainable parameter w , latent distribution $p_{Z_V}, p_{Z_A}, p_{Z_d}, p_{Z_\theta}, p_{Z_\phi}$, maximum number of atoms n

Initial: Parameters w of MolCode

- 1: **while** w is not converged **do**
- 2: Sample a batch of B molecule mol from dataset \mathcal{M}
- 3: $L = 0$
- 4: **for** $G \in mol$ **do**
- 5: Set n as the number of atoms in G and order the atoms in G
- 6: **for** $i = 1, \dots, n - 1$ **do**
- 7: Get V_i, d_i, θ_i (if $i \geq 2$), ϕ_i (if $i \geq 3$) and the reference atoms $\{f, c, e\}$
- 8: Get z_i^V, z_i^d, z_i^θ (if $i \geq 2$), z_i^ϕ (if $i \geq 3$) with the flow modules in MolCode
- 9: $L = L - \log p_{Z_V}(z_i^V) - \log p_{Z_d}(z_i^d)$
- 10: $L = L - \log p_{Z_V}(z_i^\theta)$ (if $i \geq 2$)
- 11: $L = L - \log p_{Z_V}(z_i^\phi)$ (if $i \geq 3$)
- 12: **for** $j \in \{f, c, e\}$ **do**
- 13: Get A_{ij} and z_{ij}^A
- 14: $L = L - \log p_{Z_A}(z_{ij}^A)$
- 15: **end for**
- 16: Add the binary cross entropy loss for the focal atom selection to L
- 17: **end for**
- 18: **end for**
- 19: $w \leftarrow \text{ADAM}(\frac{L}{B}, w, \eta, \beta_1, \beta_2)$
- 20: **end while**

Algorithm 2 Generation Algorithm of MolCode

Input: GoGen model with parameter w , latent distribution $p_{Z_V}, p_{Z_A}, p_{Z_d}, p_{Z_\theta}, p_{Z_\phi}$, maximum number of atoms n , maximum number of trials to sample bond types T

- 1: **for** $i = 1, \dots, n - 1$ **do**
- 2: Initialize molecular graph G_1 with one carbon atom, whose coordinate is $R_0 = [0, 0, 0]$
- 3: Sample $z_i^V \sim p_{Z_V}$ and generate V_i
- 4: Get the candidate focal atom set by the atom-wise classifier
- 5: Get the reference atoms $\{f, c, e\}$
- 6: **for** $j \in \{f, c, e\}$ **do**
- 7: Count = 0
- 8: Get $z_{ij}^A \sim p_{Z_A}$ and generate A_{ij}
- 9: **if** $\sum_j |A_{ij}| \geq \text{Valency}(X_i)$ or $\sum_i |A_{ij}| \geq \text{Valency}(X_j)$ and Count $\leq T$ **then**
- 10: Reject A_{ij} and sample a new z_{ij}^A ; Count+=1
- 11: **else**
- 12: Assign no bond to A_{ij}
- 13: **end if**
- 14: **end for**
- 15: **if** the candidate focal atom set is empty or $\sum_j |A_{ij}| = 0$ **then**
- 16: Output G_i
- 17: **else**
- 18: Random select the focal atom f from the candidate focal atom set
- 19: **end if**
- 20: Sample z_i^d, z_i^θ (if $i \geq 2$), z_i^ϕ (if $i \geq 3$)
- 21: Generate d_i, θ_i (if $i \geq 2$), ϕ_i (if $i \geq 3$) and get R_i , update G_i to G_{i+1}
- 22: **end for**
- 23: Output G_n

References (note this is the full reference list - not all are cited in the supplementary information)

1. Hajduk, P. J. & Greer, J. A decade of fragment-based drug design: strategic advances and lessons learned. *Nature reviews Drug discovery* **6**, 211–219 (2007).
2. Lawson, A. D. Antibody-enabled small-molecule drug discovery. *Nature Reviews Drug Discovery* **11**, 519–525 (2012).
3. Wang, Y., Wang, J., Cao, Z. & Barati Farimani, A. Molecular contrastive learning of representations via graph neural networks. *Nature Machine Intelligence* **4**, 279–287 (2022).
4. Freeze, J. G., Kelly, H. R. & Batista, V. S. Search for catalysts by inverse design: artificial intelligence, mountain climbers, and alchemists. *Chemical reviews* **119**, 6595–6612 (2019).
5. Gómez-Bombarelli, R. *et al.* Design of efficient molecular organic light-emitting diodes by a high-throughput virtual screening and experimental approach. *Nature materials* **15**, 1120–1127 (2016).
6. Xu, R.-P., Li, Y.-Q. & Tang, J.-X. Recent advances in flexible organic light-emitting diodes. *Journal of Materials Chemistry C* **4**, 9116–9142 (2016).
7. Polishchuk, P. G., Madzhidov, T. I. & Varnek, A. Estimation of the size of drug-like chemical space based on gdb-17 data. *Journal of computer-aided molecular design* **27**, 675–679 (2013).
8. Butler, K. T., Davies, D. W., Cartwright, H., Isayev, O. & Walsh, A. Machine learning for molecular and materials science. *Nature* **559**, 547–555 (2018).
9. Vamathevan, J. *et al.* Applications of machine learning in drug discovery and development. *Nature reviews Drug discovery* **18**, 463–477 (2019).
10. Ekins, S. *et al.* Exploiting machine learning for end-to-end drug discovery and development. *Nature materials* **18**, 435–441 (2019).
11. von Lilienfeld, O. A., Müller, K.-R. & Tkatchenko, A. Exploring chemical compound space with quantum-based machine learning. *Nature Reviews Chemistry* **4**, 347–358 (2020).
12. Westermayr, J., Gastegger, M., Schütt, K. T. & Maurer, R. J. Perspective on integrating machine learning into computational chemistry and materials science. *The Journal of Chemical Physics* **154**, 230903 (2021).
13. Zhang, Z., Liu, Q., Wang, H., Lu, C. & Lee, C.-K. Motif-based graph self-supervised learning for molecular property prediction. *Advances in Neural Information Processing Systems* **34**, 15870–15882 (2021).
14. Ceriotti, M., Clementi, C. & Anatole von Lilienfeld, O. Machine learning meets chemical physics (2021).
15. Keith, J. A. *et al.* Combining machine learning and computational chemistry for predictive insights into chemical systems. *Chemical reviews* **121**, 9816–9872 (2021).
16. Fang, X. *et al.* Geometry-enhanced molecular representation learning for property prediction. *Nature Machine Intelligence* **4**, 127–134 (2022).

- 327 17. Wang, D. *et al.* Efficient sampling of high-dimensional free energy landscapes using adaptive reinforced dynamics. *Nature Computational Science* **2**, 20–29 (2022).
- 328 18. Madani, A. *et al.* Large language models generate functional protein sequences across diverse families. *Nature Biotechnology* **1**–8 (2023).
- 329 19. Kusner, M. J., Paige, B. & Hernández-Lobato, J. M. Grammar variational autoencoder. In *International conference on machine learning*, 1945–1954 (PMLR, 2017).
- 330 20. Gómez-Bombarelli, R. *et al.* Automatic chemical design using a data-driven continuous representation of molecules. *ACS central science* **4**, 268–276 (2018).
- 331 21. You, J., Liu, B., Ying, Z., Pande, V. & Leskovec, J. Graph convolutional policy network for goal-directed molecular graph generation. In *Advances in neural information processing systems*, 6410–6421 (2018).
- 332 22. Griffiths, R.-R. & Hernández-Lobato, J. M. Constrained bayesian optimization for automatic chemical design using variational autoencoders. *Chemical science* **11**, 577–586 (2020).
- 333 23. Shi, C. *et al.* Graphaf: a flow-based autoregressive model for molecular graph generation. *International Conference on Learning Representations* (2020).
- 334 24. Gebauer, N., Gastegger, M. & Schütt, K. Symmetry-adapted generation of 3d point sets for the targeted discovery of molecules. In *Advances in Neural Information Processing Systems*, 7566–7578 (2019).
- 335 25. Wang, J. *et al.* Multi-constraint molecular generation based on conditional transformer, knowledge distillation and reinforcement learning. *Nature Machine Intelligence* **3**, 914–922 (2021).
- 336 26. Gebauer, N. W., Gastegger, M., Hessmann, S. S., Müller, K.-R. & Schütt, K. T. Inverse design of 3d molecular structures with conditional generative neural networks. *Nature communications* **13**, 1–11 (2022).
- 337 27. Zhang, Z., Min, Y., Zheng, S. & Liu, Q. Molecule generation for target protein binding with structural motifs. In *The Eleventh International Conference on Learning Representations* (2022).
- 338 28. Zhang, Z. & Liu, Q. Learning subpocket prototypes for generalizable structure-based drug design. *ICML* (2023).
- 339 29. Ma, T., Chen, J. & Xiao, C. Constrained generation of semantically valid graphs via regularizing variational autoencoders. *Advances in Neural Information Processing Systems* **31** (2018).
- 340 30. De Cao, N. & Kipf, T. Molgan: An implicit generative model for small molecular graphs. *ICML 2018 workshop on Theoretical Foundations and Applications of Deep Generative Models* (2018).
- 341 31. Zang, C. & Wang, F. Moflow: an invertible flow model for generating molecular graphs. In *Proceedings of the 26th ACM SIGKDD International Conference on Knowledge Discovery & Data Mining*, 617–626 (2020).
- 342 32. Madhawa, K., Ishiguro, K., Nakago, K. & Abe, M. Graphnvp: An invertible flow model for generating molecular graphs. *arXiv preprint arXiv:1905.11600* (2019).
- 343 33. Luo, Y., Yan, K. & Ji, S. Graphhdf: A discrete flow model for molecular graph generation. In *International Conference on Machine Learning*, 7192–7203 (PMLR, 2021).
- 344 34. Jin, W., Barzilay, R. & Jaakkola, T. Junction tree variational autoencoder for molecular graph generation. In *International conference on machine learning*, 2323–2332 (PMLR, 2018).
- 345 35. Jin, W., Barzilay, R. & Jaakkola, T. Hierarchical generation of molecular graphs using structural motifs. In *ICML*, 4839–4848 (PMLR, 2020).
- 346 36. Ganea, O. *et al.* Geomol: Torsional geometric generation of molecular 3d conformer ensembles. *Advances in Neural Information Processing Systems* **34** (2021).
- 347 37. Xu, M. *et al.* An end-to-end framework for molecular conformation generation via bilevel programming. In *International Conference on Machine Learning*, 11537–11547 (PMLR, 2021).
- 348 38. Shi, C., Luo, S., Xu, M. & Tang, J. Learning gradient fields for molecular conformation generation. In *International Conference on Machine Learning*, 9558–9568 (PMLR, 2021).
- 349 39. Liu, S. *et al.* Pre-training molecular graph representation with 3d geometry. *International Conference on Learning Representations* (2022).
- 350 40. Mahmood, O., Mansimov, E., Bonneau, R. & Cho, K. Masked graph modeling for molecule generation. *Nature communications* **12**, 1–12 (2021).
- 351 41. Hoffmann, M. & Noé, F. Generating valid euclidean distance matrices. *arXiv preprint arXiv:1910.03131* (2019).

- 375 42. Hoogeboom, E., Satorras, V. G., Vignac, C. & Welling, M. Equivariant diffusion for molecule generation in 3d. *International Conference on Machine Learning* (2022).
- 376 43. Luo, Y. & Ji, S. An autoregressive flow model for 3d molecular geometry generation from scratch. In *International Conference on Learning Representations* (2021).
- 377 44. Luo, S., Guan, J., Ma, J. & Peng, J. A 3d generative model for structure-based drug design. *Advances in Neural Information Processing Systems* **34** (2021).
- 378 45. Méndez-Lucio, O., Ahmad, M., del Rio-Chanona, E. A. & Wegner, J. K. A geometric deep learning approach to predict binding conformations of bioactive molecules. *Nature Machine Intelligence* **3**, 1033–1039 (2021).
- 379 46. Liu, M., Luo, Y., Uchino, K., Maruhashi, K. & Ji, S. Generating 3d molecules for target protein binding. *International Conference on Machine Learning* (2022).
- 380 47. Peng, X. *et al.* Pocket2mol: Efficient molecular sampling based on 3d protein pockets. *International Conference on Machine Learning* (2022).
- 381 48. Vignac, C., Osman, N., Toni, L. & Frossard, P. Midi: Mixed graph and 3d denoising diffusion for molecule generation. *arXiv preprint arXiv:2302.09048* (2023).
- 382 49. Liu, Y. *et al.* Spherical message passing for 3d graph networks. *International Conference on Learning Representations* (2022).
- 383 50. Satorras, V. G., Hoogeboom, E., Fuchs, F. B., Posner, I. & Welling, M. E (n) equivariant normalizing flows. *NeurIPS* (2021).
- 384 51. Grosnit, A. *et al.* High-dimensional bayesian optimisation with variational autoencoders and deep metric learning. *arXiv preprint arXiv:2106.03609* (2021).
- 385 52. Notin, P., Hernández-Lobato, J. M. & Gal, Y. Improving black-box optimization in vae latent space using decoder uncertainty. *Advances in Neural Information Processing Systems* **34**, 802–814 (2021).
- 386 53. Maus, N. *et al.* Local latent space bayesian optimization over structured inputs. *Advances in Neural Information Processing Systems* **35**, 34505–34518 (2022).
- 387 54. Maus, N., Wu, K., Eriksson, D. & Gardner, J. Discovering many diverse solutions with bayesian optimization. *arXiv preprint arXiv:2210.10953* (2022).
- 388 55. Papamakarios, G., Nalisnick, E., Rezende, D. J., Mohamed, S. & Lakshminarayanan, B. Normalizing flows for probabilistic modeling and inference. *Journal of Machine Learning Research* **22**, 1–64 (2021).
- 389 56. Dinh, L., Krueger, D. & Bengio, Y. Nice: Non-linear independent components estimation. *arXiv preprint arXiv:1410.8516* (2014).
- 390 57. Dinh, L., Sohl-Dickstein, J. & Bengio, S. Density estimation using real nvp. *arXiv preprint arXiv:1605.08803* (2016).
- 391 58. O’Boyle, N. M. *et al.* Open babel: An open chemical toolbox. *Journal of cheminformatics* **3**, 1–14 (2011).
- 392 59. Kim, Y. & Kim, W. Y. Universal structure conversion method for organic molecules: from atomic connectivity to three-dimensional geometry. *Bulletin of the Korean Chemical Society* **36**, 1769–1777 (2015).
- 393 60. Garcia Satorras, V., Hoogeboom, E., Fuchs, F., Posner, I. & Welling, M. E (n) equivariant normalizing flows. *Advances in Neural Information Processing Systems* **34** (2021).
- 394 61. Ramakrishnan, R., Dral, P. O., Rupp, M. & Von Lilienfeld, O. A. Quantum chemistry structures and properties of 134 kilo molecules. *Scientific data* **1**, 1–7 (2014).
- 395 62. Sun, Q. *et al.* Pyscf: the python-based simulations of chemistry framework. *Wiley Interdisciplinary Reviews: Computational Molecular Science* **8**, e1340 (2018).
- 396 63. Sun, Q. *et al.* Recent developments in the pyscf program package. *The Journal of chemical physics* **153**, 024109 (2020).
- 397 64. Anderson, A. C. The process of structure-based drug design. *Chemistry & biology* **10**, 787–797 (2003).
- 398 65. Tripathi, A. & Bankaitis, V. A. Molecular docking: from lock and key to combination lock. *Journal of molecular medicine and clinical applications* **2** (2017).
- 399 66. Alon, A. *et al.* Structures of the $\sigma 2$ receptor enable docking for bioactive ligand discovery. *Nature* **600**, 759–764 (2021).
- 400 67. Francoeur, P. G. *et al.* Three-dimensional convolutional neural networks and a cross-docked data set for structure-based drug design. *Journal of chemical information and modeling* **60**, 4200–4215 (2020).

- 422 68. Bickerton, G. R., Paolini, G. V., Besnard, J., Muresan, S. & Hopkins, A. L. Quantifying the chemical beauty of drugs.
423 *Nature chemistry* **4**, 90–98 (2012).
- 424 69. Trott, O. & Olson, A. J. Autodock vina: improving the speed and accuracy of docking with a new scoring function, efficient
425 optimization, and multithreading. *Journal of computational chemistry* **31**, 455–461 (2010).
- 426 70. Alhossary, A., Handoko, S. D., Mu, Y. & Kwoh, C.-K. Fast, accurate, and reliable molecular docking with quickvina 2.
427 *Bioinformatics* **31**, 2214–2216 (2015).
- 428 71. Landrum, G. *et al.* Rdkit: A software suite for cheminformatics, computational chemistry, and predictive modeling. *Greg
429 Landrum* **8** (2013).
- 430 72. Bento, A. P. *et al.* An open source chemical structure curation pipeline using rdkit. *Journal of Cheminformatics* **12**, 1–16
431 (2020).
- 432 73. Rappé, A. K., Casewit, C. J., Colwell, K., Goddard III, W. A. & Skiff, W. M. Uff, a full periodic table force field for
433 molecular mechanics and molecular dynamics simulations. *Journal of the American chemical society* **114**, 10024–10035
434 (1992).
- 435 74. Ragoza, M., Masuda, T. & Koes, D. R. Generating 3d molecules conditional on receptor binding sites with deep generative
436 models. *Chemical science* **13**, 2701–2713 (2022).
- 437 75. Axelrod, S. & Gomez-Bombarelli, R. Geom, energy-annotated molecular conformations for property prediction and
438 molecular generation. *Scientific Data* **9**, 1–14 (2022).
- 439 76. Peng, X., Guan, J., Liu, Q. & Ma, J. Moldiff: Addressing the atom-bond inconsistency problem in 3d molecule diffusion
440 generation. *arXiv preprint arXiv:2305.07508* (2023).
- 441 77. Steinegger, M. & Söding, J. Mmseqs2 enables sensitive protein sequence searching for the analysis of massive data sets.
442 *Nature biotechnology* **35**, 1026–1028 (2017).
- 443 78. Simm, G., Pinsler, R. & Hernández-Lobato, J. M. Reinforcement learning for molecular design guided by quantum
444 mechanics. In *International Conference on Machine Learning*, 8959–8969 (PMLR, 2020).
- 445 79. Vaswani, A. *et al.* Attention is all you need. *Advances in neural information processing systems* **30** (2017).
- 446 80. Kingma, D. P. & Ba, J. Adam: A method for stochastic optimization. *arXiv preprint arXiv:1412.6980* (2014).
- 447 81. Cowen-Rivers, A. I. *et al.* Hebo: pushing the limits of sample-efficient hyper-parameter optimisation. *Journal of Artificial
448 Intelligence Research* **74**, 1269–1349 (2022).
- 449 82. Ghose, A. K., Viswanadhan, V. N. & Wendoloski, J. J. A knowledge-based approach in designing combinatorial or
450 medicinal chemistry libraries for drug discovery. 1. a qualitative and quantitative characterization of known drug databases.
451 *Journal of combinatorial chemistry* **1**, 55–68 (1999).
- 452 83. Lipinski, C. A., Lombardo, F., Dominy, B. W. & Feeney, P. J. Experimental and computational approaches to estimate
453 solubility and permeability in drug discovery and development settings. *Advanced drug delivery reviews* **64**, 4–17 (2012).
- 454 84. Bajusz, D., Rácz, A. & Héberger, K. Why is tanimoto index an appropriate choice for fingerprint-based similarity
455 calculations? *Journal of cheminformatics* **7**, 1–13 (2015).
- 456 85. Xu, M. *et al.* Geodiff: A geometric diffusion model for molecular conformation generation. *ICLR* (2022).
- 457 86. Halgren, T. A. Merck molecular force field. v. extension of mmff94 using experimental data, additional computational data,
458 and empirical rules. *Journal of Computational Chemistry* **17**, 616–641 (1996).
- 459 87. Schütt, K. *et al.* Schnet: A continuous-filter convolutional neural network for modeling quantum interactions. In *Advances
460 in neural information processing systems*, 991–1001 (2017).
- 461 88. Schutt, K. *et al.* Schnetpack: A deep learning toolbox for atomistic systems. *Journal of chemical theory and computation*
462 **15**, 448–455 (2018).